Thermometry of Cold Atoms in Optical Lattices via Artificial Gauge Fields

Tommaso Roscilde
Laboratoire de Physique, CNRS UMR 5672, Ecole Normale Supérieure de Lyon, Université de Lyon, 46 Allée d'Italie, Lyon F-69364, France

(Received 13 September 2013; revised manuscript received 24 November 2013; published 17 March 2014)

Artificial gauge fields are a unique way of manipulating the motional state of cold atoms. Here we propose the use (practical or conceptual) of artificial gauge fields—obtained, e.g., experimentally via lattice shaking or conceptually via a Galilean transformation—to perform primary noise thermometry of cold atoms in optical lattices, not requiring any form of prior calibration. The proposed thermometric scheme relies on fundamental fluctuation-dissipation relations, connecting the global response to the variation of the applied gauge field and the fluctuation of quantities related to the momentum distribution (such as the average kinetic energy or the average current). We demonstrate gauge-field thermometry for several physical situations, including free fermions and interacting bosons. The proposed approach is extremely robust to quantum fluctuations—even in the vicinity of a quantum phase transition—when it relies on the thermal fluctuations of an emerging classical field, associated with the onset of Bose condensation or chiral order.

DOI: 10.1103/PhysRevLett.112.110403 PACS numbers: 03.75.Lm, 03.75.Hh, 07.20.Dt, 42.50.Lc

Cold atoms in optical lattices [1,2] currently represent the most prominent candidate for the quantum simulation [3] of lattice bosons and fermions, given the extreme level of tunability of the *microscopic* Hamiltonian parameters (tunneling, interaction, etc.), and the rapidly developing toolbox of experimental probes to characterize the many-body quantum state [1]. Yet, one of the most important limitations of cold-atom quantum simulation is the intrinsic difficulty to control the *macroscopic* parameters of the system, such as the chemical potential or the temperature, due to the fact that the system under investigation is virtually decoupled from any reservoir. This limitation is particularly serious if one is willing to reconstruct the equilibrium phase diagram of complex lattice Hamiltonians, study the nature of their phase transitions, etc. In particular, a proper quantum simulator should be equipped with a primary thermometric scheme, not needing any fit to theory data relative to the model of interest.

Most prominent proposals for primary thermometry of strongly interacting cold atoms [4] rely on the ability to image *in situ* the atomic cloud [5,6]. Regarding the (parabolic) trapping potential as a slowly varying external field coupling to the density, one can extract the local compressibility from the density gradient within a local-density approximation scheme and relate it to the local-density fluctuations via a fundamental fluctuation-dissipation (FD) relation, which in turn enables us to extract the temperature. This thermometry scheme (or a simplified version thereof) has been exploited in recent experiments equipped with a quantum-gas microscope [7–9]. An alternative approach, also based on high-resolution imaging and local-density approximation, implies a fit of the tails of the atomic cloud to the known thermodynamics of a diluted Bose (or Fermi) gas [10,11]. The requirement of high-resolution imaging can often be challenging in the experiments—especially when dealing with three-dimensional atomic clouds. Moreover, the above thermometry scheme completely breaks down when using box traps—which have recently become available via holographic techniques [11–13]—and which represent an important step towards the quantum simulation of bulk many-body phases.

In this Letter we propose a new thermometry scheme for optical-lattice quantum simulators, based on the use of artificial gauge fields (GF), which represent an invaluable theoretical tool, and have also recently become available in experiments [14]. In particular, a GF offers a unique way to manipulate the momentum distribution, namely, the most accessible observable in cold-atom experiments. Exploiting FD relations which link the variation of the momentum distribution upon applying an artificial GF to the noise in the momentum distribution itself, we devise a primary noise thermometer solely relying on time-of-flight measurements. Specifically, the GF necessary for thermometry can be trivial (namely, it amounts to a simple Galilean transformation of the Hamiltonian), in which case it does not even need to be realized experimentally, but it can be mimicked by a simple shift of the momentum distribution. More generally, the GF required for thermometry can be achieved via lattice shaking [15–19]—a scheme easily integrated in standard optical lattice experiments; an alternative scheme based on a combination of rf and Raman fields has been realized in Ref. [20]. We demonstrate gauge-field thermometry for a variety of physical systems, showing its robustness to the presence of strong quantum fluctuations provided that one bases thermometry on the FD relation involving an order parameter, minimally affected by quantum fluctuations.

For definiteness, let us consider the following general Hamiltonian for quantum particles in an artificial gauge field, $\mathcal{H} = \mathcal{H}_J + \mathcal{H}_U + \mathcal{H}_t$. Here,

$$\mathcal{H}_J = -J \sum_{\langle ij\rangle \| x} (e^{i\Phi} a_i^\dagger a_j + \text{H.c.}) - J \sum_{\langle lm\rangle \| \bar{x}} (a_l^\dagger a_m + \text{H.c.}) \tag{1}$$

describes the hopping between pairs of nearest-neighboring sites $\langle ij\rangle$ and $\langle lm\rangle$. In particular, we assume that the GF is introduced by the presence of a uniform Peierls phase Φ on all the bonds $\langle ij\rangle$ parallel to a given lattice direction (x), while no GF is present along the other directions ($\bar{x}$). Such a GF corresponds trivially to a Galilean transformation in the case of a square or cubic lattice, but it creates a nontrivial staggered flux in a triangular lattice [19], in a kagome lattice, etc. Furthermore, $\mathcal{H}_U$ represents an on-site interaction term, and $\mathcal{H}_t$ a trapping potential term. In the following, we will consider the case of fermionic as well as bosonic operators a, $a^\dagger$.

In our scheme, the Peierls phase Φ plays the role of the probe field. The response of a generic observable $\langle A\rangle$ ($\langle\cdots\rangle$ denoting the statistical average) to a variation of the applied GF is given by

$$\frac{\partial\langle A\rangle}{\partial\Phi} = \frac{J}{T}[\cos\Phi \,\mathrm{cov}_\tau(A, K_s) - \sin\Phi \,\mathrm{cov}_\tau(A, K_c)]. \tag{2}$$

Here, $K_c = \sum_{\langle ij\rangle \| x}(a_i^\dagger a_j + \text{H.c.})$ and $K_s = i\sum_{\langle ij\rangle \| x}(a_i^\dagger a_j - \text{H.c.})$ are, respectively, the Josephson coupling and the current operator along the x direction, and cov_τ is the (imaginary) time-averaged covariance, $\mathrm{cov}_\tau(A,B) = \frac{1}{\beta}\int_0^\beta d\tau[\langle A(0)B(\tau)\rangle - \langle A\rangle\langle B\rangle]$ ($\beta = T^{-1}$). T is the temperature. Throughout the Letter, we set $k_B = 1$.

The capability of applying a tunable GF Φ allows us to reconstruct experimentally the response function $\partial\langle A\rangle/\partial\Phi$ to the left-hand side of Eq. (2). Thermometry can be achieved through Eq. (2) if one is also able to measure the right-hand side, containing the correlation between the fluctuations of the observable A and the operators K_c, K_s—which can be extracted experimentally as discussed below. It is obvious that experiments cannot reconstruct the time-averaged covariance, but rather the conventional, equal-time one, $\mathrm{cov}(A,B) = \langle AB\rangle - \langle A\rangle\langle B\rangle$. If A (or B) commutes with the Hamiltonian, then $\mathrm{cov}_\tau(A,B) = \mathrm{cov}(A,B)$; yet for a generic optical lattice experiment, the only integrals of motion are the total particle number (which is independent of the applied GF) and the total energy (which is not easily measurable). Hence, one has to resort to a judiciously chosen observable A, whose quantum fluctuations are well controlled. We will discuss in the following how to choose such an observable. For any observable A, one has a temperature estimator T_A, which is accessible experimentally:

$$\frac{T_A}{J} =: \frac{\cos\Phi\,\mathrm{cov}(A, K_s) - \sin\Phi\,\mathrm{cov}(A, K_c)}{\partial_\Phi\langle A\rangle}. \tag{3}$$

T_A approximates arbitrarily well the temperature T of the system if the purely *quantum* fluctuations of A are arbitrarily weak. In practice this means that generic observables A related to the momentum distribution can *a priori* provide excellent estimates of the temperature in the case of a lattice Bose or Fermi gas with weak interactions, and immersed in a weakly confining potential. We will provide specific examples below—as we will see, the condition of weak interactions and confinement can, in fact, be lifted if the system develops strong correlations, robust to the presence of quantum fluctuations in the thermodynamic limit. Beyond its practical thermometry scope, the temperature estimator T_A also has a fundamental meaning: it expresses an effective temperature related to the observable A in question, accounting for its combined thermal and quantum fluctuations.

The operators K_c and K_s can be easily extracted from the momentum distribution operator $n(\boldsymbol{q}) = |w(\boldsymbol{q})|^2\sum_{ij} e^{i\boldsymbol{q}\cdot(\boldsymbol{r}_i - \boldsymbol{r}_j)} a_i^\dagger a_j$ via an inverse Fourier transform [here, $w(\boldsymbol{q})$ is the Fourier transform of the lattice Wannier function $W(\boldsymbol{r})$, $w(\boldsymbol{q}) = \int d^3r/(2\pi)^{3/2} e^{i\boldsymbol{q}\cdot\boldsymbol{r}} W(\boldsymbol{r})$]: $K_c = 2\int d^dq \cos(\boldsymbol{q}\cdot\hat{\boldsymbol{x}}) n(\boldsymbol{q})$ and $K_s = 2\int d^dq \sin(\boldsymbol{q}\cdot\hat{\boldsymbol{x}}) n(\boldsymbol{q})$. Therefore, each time-of-flight measurement realizes a projective measurement of K_c and K_s; if the observable A is also a quantity measured projectively via time of flight, a generic cold-atom experiment can access the full-counting statistics of all these quantities [21], and, in particular, the covariances contained in the temperature estimator, Eq. (3). Moreover, A should be such that $\partial_\Phi\langle A\rangle \neq 0$, and, in particular, it is convenient that the Φ dependence of $\langle A\rangle$ be significant around the value of Φ of interest.

Interacting bosons.—We begin our discussion with the case of interacting bosons undergoing a transition from a superfluid phase to a Mott insulator phase. The numerical study of the Hamiltonian with Peierls phases, Eq. (1), is notoriously difficult, given that the complex hopping amplitudes produce a negative sign problem in quantum Monte Carlo simulations. Nonetheless, in the limit of large integer filling $n \gg 1$, the Bose-Hubbard model admits a mapping onto the quantum rotor Hamiltonian [22,23]:

$$\mathcal{H}_{\mathrm{QR}} = -2Jn \sum_{\langle ij\rangle \| x} \cos(\phi_i - \phi_j - \Phi) - 2Jn \sum_{\langle lm\rangle || \bar{x}} \cos(\phi_l - \phi_m) - \frac{U}{2}\sum_i \frac{\partial^2}{\partial\phi_i^2}, \tag{4}$$

where ϕ_i is the local phase of the lattice Bose operator. Given the constraint of integer filling, the effect of trapping cannot be accurately reproduced within the quantum rotor Hamiltonian [21]—yet, we can mimic the effect of confinement by introducing open boundary conditions.

The quantum rotor Hamiltonian conveniently lends itself to path-integral Monte Carlo simulations [22], which, being formulated in the basis of the phase eigenstates, allow us to reconstruct the full-counting statistics of any quantity related to the momentum distribution, much as in time-of-flight experiments. Moreover, the quantum rotor formulation allows for the introduction of arbitrary GFs without the appearance of a sign problem. Simulations are performed on $L \times L$ square lattices and L^3 cubic lattices [21].

Square and cubic lattice.—We begin our discussion with the case of square and cubic lattices, for which the Peierls phase introduced in Eq. (1) is gauge trivial. Yet it represents an invaluable *conceptual* thermometry tool in the superfluid regime at *zero* GF for both lattices. The tool is purely conceptual because the Peierls phase induces a simple Galilean shift of the momentum distribution $n(\boldsymbol{q}) \to n(\boldsymbol{q} + \Phi\hat{x})$ [Fig. 1(c)], so that experimentally the actual application of the Peierls phase is not needed—all Φ derivatives can be evaluated by simply translating the measured momentum distribution. We consider the response of several $n(\boldsymbol{q})$-related quantities to the applied Peierls phase: (1) The already mentioned current operator K_s; (2) a measure of the asymmetry of the momentum distribution peak at $q = 0$, $D_\infty = (N_+ - N_-)/(N_+ + N_-)$, where $N_\pm = \sum_{\boldsymbol{q}\in\mathcal{D}_\pm} n(\boldsymbol{q})$ is the number of particles in a disk $\mathcal{D}_\pm$ in momentum space of radius $R = 0.4a^{-1}$ (a is the lattice spacing), centered around the point $\boldsymbol{q}_\pm = (\pm R, 0)$ [see Fig. 1(c) for an illustration] [24]; (3) the total x component of momentum in the double-disk region, $Q_{x\infty} = \sum_{\boldsymbol{q}\in\mathcal{D}_\pm} q_x n(\boldsymbol{q})/(N_+ + N_-)$, namely, the first moment (along the x direction) of the momentum distribution on the two-disk region. The three quantities are chosen so as to have a nonvanishing derivative as a function of Φ (this is not the case for K_c, which is therefore not considered here). In particular, D_∞ and $Q_{x\infty}$ are sensitive to the displacement of the $q = 0$ peak upon changing the GF [25].

Figures 1(a) and 1(b) show the temperature dependence of the thermometry relative error $\epsilon = |T_A - T|/T$ based on Eq. (3), with $A = K_s$, D_∞, and $Q_{x\infty}$ for different values of the boson-boson interaction U, up to and past the critical point for the superfluid/Mott-insulator transition—which is estimated [23] for quantum rotors on the square lattice to be $[U/(2Jn)]_c \approx 5.8$, and on the cubic lattice to be $[U/(2Jn)]_c \approx 10$. We observe that the relative error degrades as one increases the interaction, due to the enhanced quantum fluctuations in the momentum distribution. Yet the temperature dependence of ϵ is highly nonmonotonic, showing a distinct dip at intermediate temperatures, particularly marked for thermometry based on the two quantities related to the condensate peak, namely, D_∞ and $Q_{x\infty}$. At first sight this might appear surprising, as the low-temperature regime is the one in which quantum fluctuations jeopardizing the accuracy of the proposed thermometry are most prominent. On the

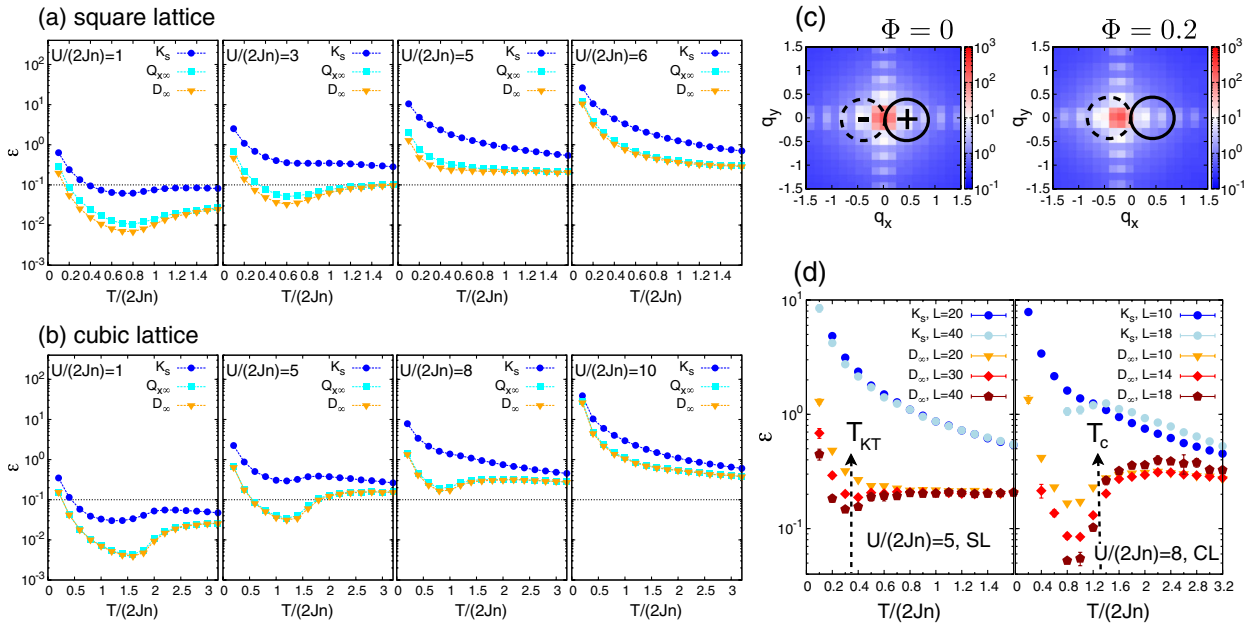

FIG. 1 (color online). Gauge-field thermometry for the quantum rotor (QR) model on the square lattice (SL) and cubic lattice (CL). (a),(b) Thermometry accuracy related to the observables K_s, $Q_{x\infty}$, and D_∞ (see text) as a function of temperature for a SL with $L = 20$ (a) and a CL with $L = 10$ (b). The dotted lines mark the 10% accuracy threshold. (c) Φ dependence of the peak position of a QR model on the SL ($L = 20$). The solid and dashed circles refer to the two contributions to D_∞. (d) Scaling of thermometry accuracy for the QR model close to the Mott insulator quantum critical point. The arrows mark the critical temperatures $T_{\mathrm{KT}}/(2Jn) = 0.34(2)$ (SL) and $T_c/(2Jn) = 1.35(5)$ (SL).

other hand, it is natural to relate this anomaly in the temperature behavior of ϵ to the phase transition of the two systems under investigation, namely, the Kosterlitz-Thouless (KT) transition of the square lattice and the condensation transition on the cubic lattice. At and below the transition, the condensate fraction becomes macroscopic (in $d = 3$) or quasimacroscopic (in $d = 2$), diverging in the thermodynamic limit, while its fluctuations (both thermal and quantum) do not follow the same scaling. This means that thermometry related to fluctuations of the condensate peak can be expected to be minimally affected by quantum fluctuations. In particular, as shown in Fig. 1(d), upon increasing the size of the system, the accuracy of thermometry *improves* with growing system size below the KT transition in $2d$ ($T < T_{\mathrm{KT}}$) and below the condensation transition in $3d$ ($T < T_c$). A detailed scaling analysis [21] shows that the relative error ϵ of thermometry associated with D_∞ appears to scale as L^{-1} below the KT transition in $2d$ and as $(L \log L)^{-1}$ below the condensation transition in $3d$, as a result of the scaling of the covariance difference $\Delta\mathrm{cov}(D_\infty, K_s) = \mathrm{cov}(D_\infty, K_s) - \mathrm{cov}_\tau(D_\infty, K_s)$, as well as of the derivative $\partial_\Phi D_\infty$ (the latter showing agreement with Bogolyubov theory). On the other hand, the relative error ceases to scale in the normal phase.

Triangular lattice with a π flux.—As a second example, we consider thermometry in a system with an applied, nontrivial GF, namely, a triangular lattice with a π flux, realized recently via lattice shaking in Refs. [17,19]. Such a system possesses an additional, discrete Z_2 symmetry associated with the choice of two degenerate vortex patterns (with alternation of vortices or antivortices on adjacent plaquettes, Fig. 2(b) [26]). This symmetry is broken via a chiral Ising transition at a critical temperature T_k, as also observed in the experiments [17,19]. In particular, the two vortex patterns can be distinguished by the appearance of a finite current K_s on the horizontal links of the triangular lattice, serving, therefore, as an order parameter [Fig 2(b)]. Figures 2(a) and 2(c) show the accuracy of thermometry based on K_s as a function of temperature and of increasing repulsion U among the bosons. For $U > U_c \approx 2.8(2Jn)$, the repulsion drives the system across a quantum critical point with destruction of long-range chiral order [27]. Yet we observe that, similarly to the condensation transition of the previous example, the chiral transition boosts the accuracy of thermometry in a dramatic fashion up to the quantum critical point. In particular, in the chiral phase the relative error of the proposed thermometry scales as L^{-2}, driven by the very violent divergence of $\partial_\Phi \langle K_s \rangle$ (as L^4) [21].

Free fermions on the triangular lattice.—We end our discussion by illustrating the thermometry scheme in question in the case of free fermions ($\mathcal{H}_U = 0$). In the absence of a trapping potential, the Hamiltonian commutes with K_c and K_s, so that $T_{K_c} = T_{K_s} = T$. Yet the presence of a trapping potential term, $\mathcal{H}_t = V \sum_i [(\boldsymbol{r}_i - \boldsymbol{r}_0)/a]^2 n_i$ (with a the lattice spacing), induces quantum fluctuations in the K_s and K_c operators, giving rise to a discrepancy between the above temperature estimators and the actual temperature. To evaluate the impact of quantum fluctuations, we consider a diluted fermionic system of $N = 50$ fermions on a triangular lattice, subject to a confining potential $V = 0.1J$. Figure 3 shows exact diagonalization results [21] for the temperature estimators: we observe that, for most values of the flux Φ, both T_{K_c} and T_{K_s} lie very close to the actual temperature, and that the relative error ϵ is typically $< 10\%$ for $T > 0.1 T_F$; we anticipate a significantly better accuracy of the temperature estimators for systems that experience a weaker confining potential, or are trapped in a steeper than parabolic trap. It is important to observe that T_{K_s} has a sharp singularity at $\Phi = \pi/2$, due to the fact that $\partial_\Phi \langle K_s \rangle$ vanishes at that value. On the other hand, $\partial_\Phi \langle K_c \rangle = 0$ for $\Phi = 0, \pi$. Therefore, the two temperature estimators are fully complementary [28].

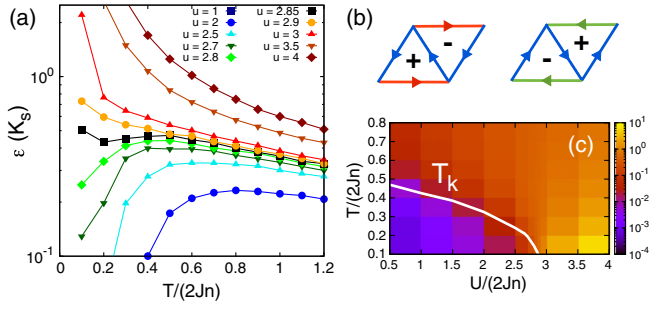

FIG. 2 (color online). Gauge-field thermometry for the QR model on a triangular lattice with a π flux. (a) T dependence of the accuracy of thermometry based on the current K_s for different interactions $u = U/(2Jn)$ crossing the quantum critical point $u_c \approx 2.8$. (b) Degenerate vortex patterns in the ground state of the model. (c) Phase diagram of the model, with comparison between the chiral transition temperature T_k and the $\varepsilon(K_s)$ accuracy (false colors).

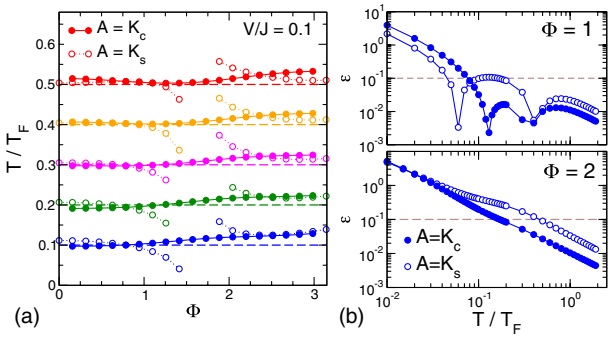

FIG. 3 (color online). Gauge-field thermometry for free fermions on a triangular lattice. (a) Estimated temperatures for $N = 50$ fermions in a trapping potential $V/J = 0.1$ as a function of the staggered flux Φ. (b) Relative error of the temperature estimator, $\epsilon = (T_A - T)/T$, as a function of temperature and for two different Φ values—other parameters as in (a). The horizontal dashed line marks the 10% accuracy threshold.

In conclusion, we propose gauge-field thermometry for cold atoms in optical lattices, namely, primary thermometry based on monitoring the fluctuations of the momentum distribution, as well as its response to the application of an artificial gauge field (either trivial or actually realized in the experiment). The proposed thermometry paves the way for the reconstruction of the phase diagram of fundamental lattice models using cold-atom quantum simulators. Future work [27] will address the extension of this scheme to continuum space as well as to disordered systems.

Stimulating discussions with J. Simonet, F. Gerbier, and especially A. Eckardt are gratefully acknowledged, as well as support from the PSMN (ENS Lyon), where all calculations were performed. This work is supported by the ANR-JCJC project "ArtiQ", and by the Institut Universitaire de France.

[1] I. Bloch, J. Dalibard, and W. Zwerger, Rev. Mod. Phys. **80**, 885 (2008).
[2] M. Lewenstein, A. Sanpera, and V. Ahufinger, *Ultracold Atoms in Optical Lattices: Simulating Quantum Many-Body systems* (Oxford University Press, Oxford, 2012).
[3] For recent surveys, see I. Buluta and F. Nori, Science **326**, 108 (2009); Nat. Phys. **8**, 4 (2012); I. M. Georgescu, S. Ashhab, and F. Nori, Rev. Mod. Phys. **86**, RB10040 (2014).
[4] D. C. McKay and B. DeMarco, Rep. Prog. Phys. **74**, 054401 (2011).
[5] Q. Zhou and T.-L. Ho, Phys. Rev. Lett. **106**, 225301 (2011).
[6] P. N. Ma, L. Pollet, and M. Troyer, Phys. Rev. A **82**, 033627 (2010).
[7] C. Sanner, E. J. Su, A. Keshet, R. Gommers, Yong-il Shin, W. Huang, and W. Ketterle, Phys. Rev. Lett. **105**, 040402 (2010).
[8] T. Müller, B. Zimmermann, J. Meineke, J.-P. Brantut, T. Esslinger, and H. Moritz, Phys. Rev. Lett. **105**, 040401 (2010).
[9] A. Vogler, R. Labouvie, F. Stubenrauch, G. Barontini, V. Guarrera, and H. Ott, Phys. Rev. A **88**, 031603(R) (2013).
[10] Yong-il Shin, C. H. Schunck, A. Schirotzek, and W. Ketterle, Nature (London) **451**, 689 (2008).
[11] J. F. Sherson, C. Weitenberg, M. Endres, M. Cheneau, I. Bloch, and S. Kuhr, Nature (London) **467**, 68 (2010).
[12] W. S. Bakr, J. I. Gillen, A. Peng, S. Foelling, and M. Greiner, Nature (London) **462**, 74 (2009).
[13] A. L. Gaunt, T. F. Schmidutz, I. Gotlibovych, R. P. Smith, and Z. Hadzibabic, Phys. Rev. Lett. **110**, 200406 (2013).
[14] J. Dalibard, F. Gerbier, G. Juzeliunas, and P. Öhberg, Rev. Mod. Phys. **83**, 1523 (2011);N. Goldman, G. Juzeliunas, P. Öhberg, and I. B. Spielman, arXiv:1308.6533.
[15] H. Lignier, C. Sias, D. Ciampini, Y. Singh, A. Zenesini, O. Morsch, and E. Arimondo, Phys. Rev. Lett. **99**, 220403 (2007).
[16] E. Arimondo, D. Ciampini, A. Eckardt, M. Holthaus, and O. Morsch, Adv. At. Mol. Opt. Phys. **61**, 515 (2012).
[17] J. Struck, C. Ölschläger, R. Le Targat, P. Soltan-Panahi, A. Eckardt, M. Lewenstein, P. Windpassinger, and K. Sengstock, Science **333**, 996 (2011).
[18] J. Struck, C. Ölschläger, M. Weinberg, P. Hauke, J. Simonet, A. Eckardt, M. Lewenstein, K. Sengstock, and P. Windpassinger, Phys. Rev. Lett. **108**, 225304 (2012).
[19] J. Struck, M. Weinberg, C. Ölschläger, P. Windpassinger, J. Simonet, K. Sengstock, R. Höppner, P. Hauke, A. Eckardt, M. Lewenstein, and L. Mathey, Nat. Phys. **9**, 738 (2013).
[20] K. Jiménez-García, L. J. LeBlanc, R. A. Williams, M. C. Beeler, A. R. Perry, and I. B. Spielman, Phys. Rev. Lett. **108**, 225303 (2012).
[21] See Supplemental Material athttp://link.aps.org/supplemental/10.1103/PhysRevLett.112.110403 for a detailed discussion of (1) the effects of a finite momentum resolution in the experiments; (2) the exact diagonalization of non-interacting fermions; (3) the quantum Monte Carlo simulation of quantum rotors; (4) the scaling of the relative error of thermometry for interacting bosons; (5) the effect of a confining potential in the case of interacting bosons.
[22] M. Wallin, E. S. Sorensen, S. M. Girvin, and A. P. Young, Phys. Rev. B **49**, 12115 (1994).
[23] N. Teichmann, D. Hinrichs, M. Holthaus, and A. Eckardt, Phys. Rev. B **79**, 100503 (2009).
[24] In the case of a cubic lattice the $\mathcal{D}_{\pm}$ regions are actually cylinders in the three-dimensional momentum space, because we also account for integration along the line of sight (z direction).
[25] Note that the height of the condensate peak is insensitive to the gauge field around $\Phi = 0$, as the peak width is independent of Φ, while the momentum occupation at $q = 0$ attains a maximum for $\Phi = 0$.
[26] D. H. Lee, J. D. Joannopoulos, J. W. Negele, and D. P. Landau, Phys. Rev. Lett. **52**, 433 (1984); S. E. Korshunov, Phys. Usp. **49**, 225 (2006).
[27] T. Roscilde (unpublished).
[28] The existence of vanishing points for the above derivatives are expected by general symmetry arguments; nonetheless, an experiment should be able to detect the poor accuracy of a temperature estimator from the strong decrease in the derivative of the associated observable.